Initial Attempt on Wi-Fi CSI Based Vibration Sensing for Factory Equipment Fault Detection

Sirui Jian*
ISEE, Kyushu University
Fukuoka, Japan

Shigemi Ishida†
ISEE, Kyushu University
Fukuoka, Japan

Yutaka Arakawa†
ISEE, Kyushu University
Fukuoka, Japan

ABSTRACT

Wi-Fi signal based detection is widely implemented in indoor action detection because of its low-cost and easy implementation. But it is still rarely used in equipment vibration detection. Moreover, it is hard to detect multiple targets where we need to monitor multiple equipments' vibration state such as in the factory environment. In this paper, we propose a wireless based vibration sensing method using Wi-Fi for factory equipment fault detection. First, we use CSI amplitude data to distinguish sensing target equipments. Then, we apply an anomaly detection method to detect faulty machine operation. We conducted initial experiments to validate the feasibility of our proposed fault detection method. The experimental results show that our method detected abnormal situations with an accuracy of 100%, while 10% of normal situations were mistakenly recognized as abnormal.

CCS CONCEPTS

• **Hardware** → **Sensors and actuators**; **Wireless integrated network sensors**.

KEYWORDS

Channel state information (CSI), commodity Wi-Fi, vibration sensing, anomaly detection.

ACM Reference Format:
Sirui Jian, Shigemi Ishida, and Yutaka Arakawa. 2021. Initial Attempt on Wi-Fi CSI Based Vibration Sensing for Factory Equipment Fault Detection. In *Adjunct Proceedings of the 2021 International Conference on Distributed Computing and Networking (ICDCN '21), January 5–8, 2021, Nara, Japan.* ACM, New York, NY, USA, 6 pages. https://doi.org/10.1145/3427477.3429462

1 INTRODUCTION

The development of modern sensing technology towards digitalization and information has become an inevitable development trend in the highly developed modern industry. The forefront of the detection system is a sensor, which is the soul of the entire sensing system. In these decade, certain companies use high-end technologies such as combination of microphone and camera to keep detecting the factory equipment's condition. In this paper, we focus on the vibration of equipments because equipments are in a vibrate condition when it is working.

Vibration sensors play an important role in the sensing system. Vibration sensors measure equipments' vibration frequency. When the equipment works in a bad condition, vibration sensors will get the outlier frequency and execute the next command to protect equipments. Motivated by this, we propose a low-cost factory equipment fault detection system based on Wi-Fi.

Although a large number of vibration sensors are active sensors, in this paper, we propose a passive vibration sensor based on wireless signal. Active vibration sensors need regular maintenance, in conclusion, the active vibration sensor is working in a high-cost situation. We develop a low-cost and more efficient sensing system to reduce the electric and maintenance costs.

In this research, our key idea is exploit the Wi-Fi channel state information (CSI) to detect the vibration. Wi-Fi is a low-cost and large-scale deployment technology that could be implemented everywhere. Wi-Fi orthogonal frequency division multiplexing (OFDM) communication [6] with a multiple-input multiple-output (MIMO) technique [2] calculates radio channel response on many subcarriers for communication, which can be derived as CSI on IEEE 802.11n/ac compliant devices. Wi-Fi CSI-based detection methods have been successfully applied to many indoor environment applications, such as fall detection [10], metal detection [12], danger-pose detection [14]. These applications capture a human's or object's motions/actions which have the big range of movements or oblivious feature that can easily affect the Wi-Fi CSI. Also, existing Wi-Fi CSI-based work on indoor recognition is predominantly consider single object scenarios, in other words, they cannot be deployed in a multiple target situation.

As we know, it is not only one equipment in the factory, for detecting the equipment's vibrate condition in factory, we face three problems.

- It is difficult to get the changing features of the vibration frequency because the noise or the human motion can cover the vibration details easily.
- It is not only one equipment in the factory. We need to recognize equipment that needs to be monitored.

ICDCN '21, January 5–8, 2021, Nara, Japan

ACM ISBN 978-1-4503-8184-0/21/01…$15.00
https://doi.org/10.1145/3427477.3429462

- For equipment fault detection, we can only rely on normal operation data because it is unrealistic to collect abnormal operation data.

Our goal is to detect abnormal vibration conditions of the vibrating equipment and show the possibility of monitoring multiple vibrating equipments at the same time. Toward this goal, we use different types of patch antennas attached to factory machines to detect the vibration of different targets. Inspired by 3D printing Wi-Fi [4], different types of patch antennas will have different power influence on Wi-Fi CSI. We therefore utilize different antennas to extract vibration information for each machine and then utilize an anomaly detection algorithm that requires only normal data of the vibration of the equipment for fault detection.

The main contributions of this paper are as follows:

- To recognize equipments, we propose to use a Wi-Fi patch antenna as an identity tag which will be attached to a vibration machine. Based on a backscatter phenomenon, different types of Wi-Fi patch antennas can reflect CSI in different. In this paper, we use two types of Wi-Fi patch antennas and show the possibility of monitoring multiple vibrating equipments at the same time.
- We conduct experiments and show that our fault detection system recognized abnormal frequency situation as anomaly with an accuracy of 100%, while 10% of normal situations were mistakenly recognized as abnormal.
- We also validated that our fault detection system classifies four kinds of vibration frequency based on the Wi-Fi CSI with an accuracy of 88%.

The rest of this paper is organized as follows. In Section 2, we review related work. The fault detection system is described in Section 3, followed by experimental details and performance evaluation in Section 4. In Section 5, we conclude the paper with some highlights of the future work.

2 RELATED WORK

In this section, we review related works on traditional vibration sensor and indoor detecting with Wi-Fi CSI.

2.1 Traditional Vibration Sensor

Most of the traditional vibration sensors require power supply. The most traditional sensors are required to be extremely sensitive to vibration, and have strong robustness and durability, so they all has a very complex structure [1]. The equipment monitoring system consists of not only vibration sensors, but also a framework for collecting and analyzing vibration information to monitor the operating conditions of the equipment. Therefore, maintaining this analysis framework is also very important [5]. In summary, a complete set of traditional equipment detection system not only requires the cost of the vibration sensor itself, but also requires power supply and additional maintenance costs.

2.2 CSI-Based Indoor Detection

Recently, Wi-Fi CSI-based system have been broadly used for indoor sensing. The Wi-Fi CSI based sensing systems are low-cost and can be implemented easily as the system needs no specialized infrastructure. Wi-metal [12], for example, employs the Wi-Fi CSI amplitude values for recognizing different kinds of metal. The Wi-Fi CSI sensing is also used in the indoor health care such as Wi-Fall [10], which utilizes CSI to detect human falling motion in indoor environments. Danger-pose detection [14] in bathroom monitors human motion in the privacy situation, which employs an anomaly detection algorithm to avoid collecting the danger pose data. The Wi-wheat [13] employs CSI to classify the wheat moisture content through the SVM classifier, showing the possibility to classify the small changes in the target.

These are examples of Wi-Fi indoor human activity monitoring and static target classification. There are very few examples of using Wi-Fi signals to monitor vibration targets. ART utilizes Wi-Fi signals to eavesdrop the audio from speakers [11]. The basic idea of ART lies in an acoustic-radio transformation algorithm, which restores the sound of the speaker by examining the CSI changes affected by speaker metal component. 3D printing Wi-Fi [4] uses a 3D printed backscatter module to affect the Wi-Fi signal when the module changes its condition. Although these methods successfully realized CSI-based vibration sensing, multiple targets are not in consideration.

3 VIBRATION SENSOR FOR FACTORY EQUIPMENT FAULT DETECTION SYSTEM

3.1 System Overview

Figure 1 illustrates a Wi-Fi CSI-based vibration sensor for factory equipment fault detection system. The CSI based vibration sensor consists of four blocks: CSI acquisition, pre-process, target identifying, and fault detection blocks. We first set up vibrators with a different type of patch antennas attached. A data acquisition block consists of a Wi-Fi transmitter and receiver, where CSI data is collected. The collected CSI data is passed to a pre-processing block, which performs amplitude extraction and applies a band-pass filter to denoise unnecessary noise components. Finally, to focus on the vibrating, we perform background subtraction to move out the static environment content. In a target identifying block, we utilize a classifier to distinguish target machine based on the patch antenna attached to each machine. Then we apply an anomaly detection algorithm in fault detection block to detect faulty situations.

Following subsections present details of each block.

3.2 CSI Acquisition Block

Our fault detection system utilizes Wi-Fi CSI to monitor the vibration status of multiple equipment. Wi-Fi not only adopts OFDM technique in the physical layer, but also makes full use of MIMO with IEEE 802.11n/ac in most existing commodity

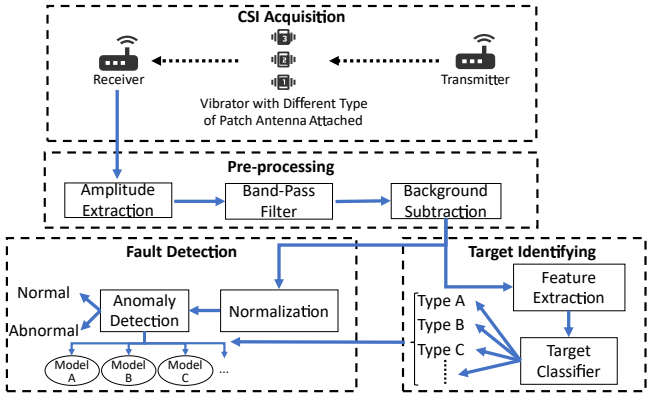

Figure 1: Overview of Wi-Fi CSI based vibration sensor for factory equipment fault detection system.

Wi-Fi devices. In OFDM, the entire spectrum (for example, 20MHz or 40MHz in IEEE 802.11n) is divided into multiple orthogonal subcarriers [8, 9]. In 802.11n/ac, each MIMO link includes multiple subcarriers and each subcarrier has an independent channel frequency response characterized by CSI. CSI means Channel State Information, which illustrates the channel frequency response of each subcarrier in the OFDM. The channel frequency response of the i-th subcarrier can be written as

$$h_i = |h_i| \exp \angle h_i, \tag{1}$$

where $|h_i|$ denotes the amplitude and $\angle h_i$ denotes the phase information for the i-th subcarrier.

In our fault detection system, we exploit a different type of patch antennas as identity tags for target identification because they will have different reflection to channel frequency response $|h_i|$. We leverage CSI amplitude $|h_i|$ for fault detection since the amplitude $|h_i|$ will have great alter between different patch antennas.

3.3 Pre-Processing Block

As shown in Fig. 1, the pre-processing block consists of amplitude extraction, band-pass filter, and background subtraction sub-blocks.

In an amplitude extraction sub-block extracts CSI amplitude difference data for equipment vibration fault detection. We utilize CSI tool [3] that derive CSI from an Intel Wi-Fi Link 5300 NIC. Although 802.11n uses at least 52 subcarriers, we can only derive CSI for 30 subcarriers using CSI tool. We extract the amplitude in the raw CSI which extracted by the CSI tool as a complex number as shown in Equation (1).

In a band-pass filter sub-block, we apply a band-pass filter to reduce random noise embedded in the received CSI data packets. To improve the efficiency of the experiment and get more data packets within a certain period of time, we set the data packet sampling rate to 100Hz. According to the sampling theorem, a series of time-varying CSI contains frequency components from 0 to $(F_s/2)$ Hz, where F_s is a sampling frequency. Since human activities usually include low-frequency content [7] and the sampling frequency F_s is much greater than the maximum vibration frequency of the vibrator used in our experiments, many redundant high-frequency noises will be generated. We used a brush-less direct current (DC) motor in our experiment. The DC motor work within a frequency range of 0–15Hz. We set the lower and upper cut-off frequencies of the band-pass filter as 4 and 16Hz, respectively. We use a Butterworth band-pass filter at subcarrier level to eliminate low-frequency content caused by human activities and high-frequency noise.

In a background subtraction sub-block, we focus on the CSI changes brought by the vibration of the vibrator. The CSI information not only includes vibration information of the vibrator, but also environmental information. As the Wi-bath danger pose detection [14] pointed out, among different receiving antennas, the CSI difference of the same subcarrier is sensitive to activity, but not sensitive to environmental changes. We use the CSI difference between the receiving antennas instead of directly using CSI for background subtraction.

Here we describe $\widetilde{CSI}(t)$ using channel frequency response of each reception antenna:

$$\widetilde{CSI}(t) = [\widetilde{H}_{1,1}(t), \cdots, \widetilde{H}_{1,30}(t), \widetilde{H}_{2,1}(t), \cdots, \widetilde{H}_{2,30}(t)], \tag{2}$$

where $\widetilde{H}_{m,n}$ is the band-pass filtered channel response of Equation (1) for subcarrier n on reception antenna m.

In this work, we only used two antennas due to the limitation of the devices used in our experiment. We can calculate the difference $CSI'(t)$ as:

$$CSI'(t) = [\widetilde{H}_{2,1}(t) - \widetilde{H}_{1,1}(t), \cdots, \widetilde{H}_{2,30}(t) - \widetilde{H}_{1,30}(t)]. \tag{3}$$

3.4 Target Identifying Block

The target identifying block consists of feature extraction and target classifier sub-blocks.

A feature extraction block first extracts features from the pre-processed CSI data, as shown in Fig. 1. As a feature, we calculate standard deviation of each subcarrier in a fixed length window. Feature values are calculated over the fixed length window, which is slid with no overlap, as shown in Fig. 2.

For example, if the slide window size $w = 100$, the feature extraction process is as follows. (1) We split pre-processed CSI data into data chunks at a length of 100 for each subcarrier. The first chunk is $[CSI'(0), \cdots, CSI'(99)]$, and the second chunk is $[CSI'(100), \cdots, CSI'(199)]$, etc. (2) We calculate standard deviation of each chunk.

In a target classifier sub-block, feature vectors, consisting of standard deviation of subcarriers, are fed into a supervised target classifier. We don't limit the classifier algorithm. In this paper, we utilize a random forest classifier to distinguish the type of patch antennas.

3.5 Fault Detection Block

The fault detection block exploits anomaly detection algorithm to identify the normal vibration state and abnormal vibration state of the different equipment. Although there

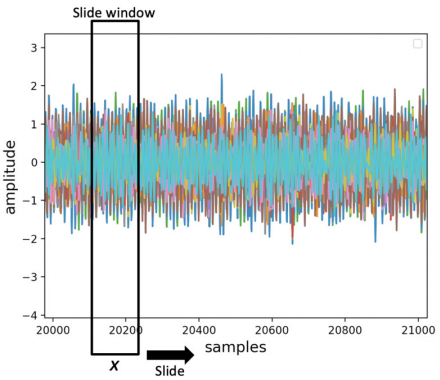

Figure 2: Example of slide windowing.

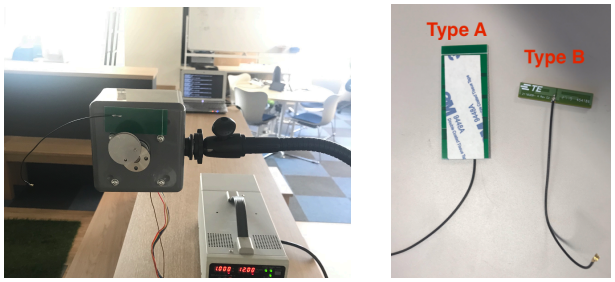

(a) (b)

Figure 3: Experiment setup: (a) vibrator, (b) two types of patch antennas.

are many algorithm of the anomaly detection, we utilize the one-class support vector machine (SVM). Gaussian Radial Basis Function (RBF) is used as the kernel.

In the fault detection block, the first process is to load a machine learning model based on the result of target identifying. For example, we load the model for type A antenna when the target identifying result is type A.

We then operate a normalization process in order to achieve high detection performance. Note that the fault detection block uses difference CSI given in Eq. (3) instead of standard deviation over sliding window calculated in Section 3.4. The normalized value Y_i for a fault detection classifier is calculated as:

$$Y_i = \frac{X_i - X_{mean}}{X_{max} - X_{min}}, \tag{4}$$

where X_i represents a value in difference CSI given in Eq. (3), X_{mean}, X_{max}, and X_{min} are the average, maximum, and minimum of difference CSI in training data set, respectively.

We train a one-class SVM classifier model with CSI data collected under the normal working frequency. In our fault detection system, we regard that the machine is in abnormal operation when the working frequency is outside of frequencies labeled as normal.

4 EXPERIMENT

We conducted experiments in an indoor line-of-sight (LOS) environment with no human.

4.1 Experiment Environment

Figure 3 shows an experiment setup. We installed two Toshiba dynabook laptops equipped with Intel 5300 NIC as a Wi-Fi transmitter and receiver at a distance of 4 meters. A vibration machine was installed in the middle of the transmitter and receiver. The vibration machine was implemented with a TP-3641EB-CM-5-H00-12 brush-less DC motor. Eccentric motor coupling made from iron was attached to the motor shaft to enhance vibration. The motor's working frequency is in a range of 0–15Hz, which can be controlled from a controlling micro-controller board. The DC motor is supported dy a flexible camera arm not to disturb vibration. Note that there was no human around this testing field during the experiment.

We attached two types of patch antennas, type A and B, to the vibrator and collected CSI data while the vibrator motor operated in 0, 5, 10, and 15Hz. CSI data while no patch antenna attached was also collected. We name CSI data sets as $\mathbf{Z}_f$, where $\mathbf{Z} \in \{\mathbf{A}, \mathbf{B}, \mathbf{None}\}$ represent antenna type and $f \in \{0, 5, 10, 15\}$ represents operating frequency in Hertz. For example, $\mathbf{A}_{10}$ denotes the set of CSI data collected while the vibrator motor operated in 10Hz with the type A antenna attached. Type **None** corresponds to no antenna situation. We also define an aggregated sets as:

$$\mathbf{Z} = \bigcup_{f \in \{0,5,10,15\}} \mathbf{Z_f}. \tag{5}$$

We collected CSI data for 20 minutes in each condition with a sampling frequency of 100Hz. The length of CSI data is therefore 120,000, i.e., $|\mathbf{Z}_f| = 120000$.

4.2 Target Identifying Performance

We first evaluated target identifying performance. From datasets **A**, **B**, and **None**, we derived feature vectors, i.e., standard deviation of each subcarrier in each window. The sliding window size w defined in Section 3.4 was set to 100. We therefore derived 1,200 feature vectors for each subcarrier in each of **A**, **B**, and **None** situations. Note that the size of each feature vector is 30 because we derive CSI data using 802.11n CSI tool that only provides CSI for 30 subcarriers. We took 80% of feature vectors for training the target identifying model and tested the performance with the remaining 20% of data.

Figure 4 shows a confusion matrix of target identifying result. Figure 4 indicates that target identifying method successfully identified antenna type with a recall of 88.1% and with an F1 score of 88.2%. This result indicated the possibility of equipment identification using different types of patch antenna.

4.3 Fault Detection Performance

We next evaluated fault detection performance. In this evaluation, we assume that the machine is abnormal when the

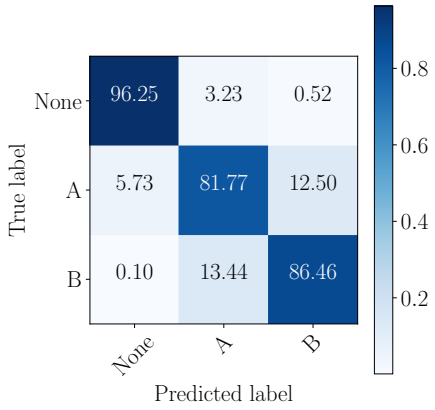

Figure 4: Confusion matrix of target identifying classification result.

vibrator stops, i.e., operating in 0Hz. We therefore put the label 'abnormal' to $\mathbf{Z}_0$ and the label 'normal' to $\bigcup_{f\in\{5,10,15\}} \mathbf{Z}_f$, where $\mathbf{Z} \in \{\mathbf{A}, \mathbf{B}\}$. Note that we ignored the dataset **None** as we don't monitor faulty status when no antenna is attached to machines.

As described in Section 3.5, we trained the fault detection model for each type of antennas. The fault detection performance was evaluated with the assumption that the target identifying process successfully identified antenna types. For each model, we took 80% of $\mathbf{Z}_f$ for training and tested with the remaining 20% of the data.

Figure 5 shows confusion matrices of fault detection result for type A and B antennas. From Fig. 5, we can confirm that our fault detection system detected abnormal situations with an accuracy of 100%, while 10% of normal situations were mistakenly detected as 'abnormal'. We found no influence of antenna difference in this experiment.

4.4 Fault Detection Performance When Target Identifying Failed

Remind that the target identifying performance, presented in the previous subsection, was also not 100% accuracy. Referring to Fig. 4, for example, type A antenna was classified into type B antenna for 12.50%. In this situation, type A antenna data will be fed into type A fault detection model.

We evaluated the fault detection performance in these situations. We trained fault detection model with the data for one type of antenna and tested with the data for another antenna. For type A model test, for example, we trained the fault detection model with a dataset **A** and tested with **B**. 'Normal' and 'abnormal' labels were given in the same manner as described above.

The results were all the same: all trials fell into 'abnormal'. Fault detection performance was also evaluated with a dataset of **None**, which also fell into 'abnormal'. These results are natural because data for different antenna type was not fed into fault detection model for training as 'normal'. We can

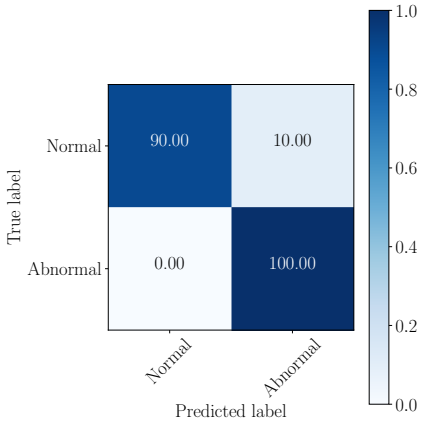

(a)

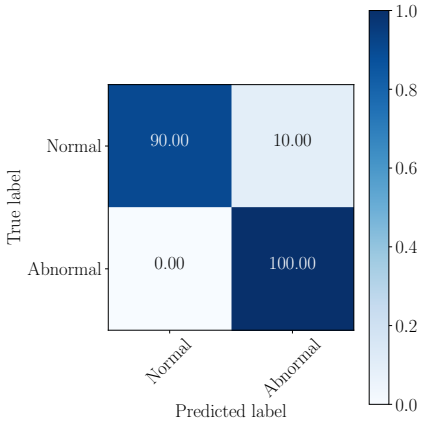

(b)

Figure 5: Confusion matrix of fault detection result for (a) type A and (b) type B antennas.

conclude that target identifying performance has significant influence on fault detection performance. We therefore need to more improve target identifying performance.

4.5 Frequency Identification Performance

In machine operation monitoring, frequency monitoring is also useful. We therefore evaluated operating frequency identification performance as a supplement. We directly fed difference CSI into a random forest classifier to identify operating frequency $f \in \{0, 5, 10, 15\}$. In the same manner as in the fault detection block, the frequency identification classifier was separately trained for each type of antennas. We took 80% of data for training and tested with the remaining 20% of the data.

Figure 6 shows confusion matrices of frequency identification result for type A and B antennas. From Fig. 6, we can confirm that our fault detection system identified operating

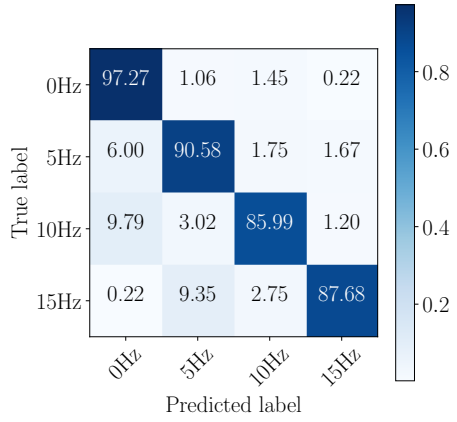

(a)

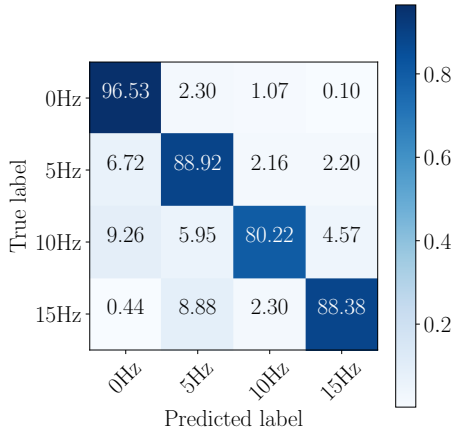

(b)

Figure 6: Confusion matrix of frequency identification result for (a) type A and (b) type B antennas.

frequency with an average accuracy of 90.38% and 88.51% for type A and B antennas, respectively. These results indicated that the Wi-Fi CSI could be used not only for fault detection, but also for vibration frequency sensing.

5 CONCLUSION AND FUTURE WORK

In this paper, we presented an initial attempt on Wi-Fi CSI based vibration sensing method for factory equipment fault detection. Our system performs two-step estimation: identifies different type of patch antennas and then performs equipment fault detection. There are multiple equipments in a factory. We therefore first identifies a target equipment using patch antenna and then focus on the target for fault detection. As we can only derive normal operation data, we employ anomaly detection method for fault detection. Experimental results revealed that our fault detection system successfully detected abnormal situations with an accuracy of 100%, while 10% of normal situations were mistakenly detected as abnormal.

Our initial attempt used a single vibrator and different type of patch antenna to show the possibility of monitoring multiple targets by Wi-Fi CSI. As CSI is sensitive to the changes of a surrounding environment, we conducted our experiment where no human was around. We also used transmitter, receiver, and vibrator at fixed locations in our experiment. In a practical environment, the surrounding environment is always changed. Therefore, in the future work, we will design a method to reduce the influence of a surrounding environment and improve target detection performance. Moreover, we will conduct experiments with multiple vibrators with different types of patch antenna.

ACKNOWLEDGMENTS

This work is supported in part by JSPS KAKENHI Grant Numbers JP18K18041 and JP19KK0257.

REFERENCES

[1] Jonathan Bernstein, Raanan Miller, William Kelley, and Paul Ward. 1999. Low-noise MEMS vibration sensor for geophysical applications. *Journal of microelectromechanical systems* 8, 4 (1999), 433–438.

[2] Lai-U Choi and Ross D Murch. 2004. A transmit preprocessing technique for multiuser MIMO systems using a decomposition approach. *IEEE Transactions on Wireless Communications* 3, 1 (2004), 20–24.

[3] Daniel Halperin, Wenjun Hu, Anmol Sheth, and David Wetherall. 2011. Tool release: Gathering 802.11 n traces with channel state information. *ACM SIGCOMM Computer Communication Review* 41, 1 (2011), 53–53.

[4] Vikram Iyer, Justin Chan, and Shyamnath Gollakota. 2017. 3D printing wireless connected objects. *ACM Transactions on Graphics (TOG)* 36, 6 (2017), 1–13.

[5] Deokwoo Jung, Zhenjie Zhang, and Marianne Winslett. 2017. Vibration analysis for iot enabled predictive maintenance. In *2017 IEEE 33rd International Conference on Data Engineering (ICDE)*. IEEE, 1271–1282.

[6] Richard van Nee and Ramjee Prasad. 2000. *OFDM for wireless multimedia communications*. Artech House, Inc.

[7] Guanhua Wang, Yongpan Zou, Zimu Zhou, Kaishun Wu, and Lionel M Ni. 2016. We can hear you with Wi-Fi! *IEEE Transactions on Mobile Computing* 15, 11 (2016), 2907–2920.

[8] Xuyu Wang, Lingjun Gao, Shiwen Mao, and Santosh Pandey. 2016. CSI-based fingerprinting for indoor localization: A deep learning approach. *IEEE Transactions on Vehicular Technology* 66, 1 (2016), 763–776.

[9] Xuyu Wang, Chao Yang, and Shiwen Mao. 2017. TensorBeat: Tensor decomposition for monitoring multiperson breathing beats with commodity WiFi. *ACM Transactions on Intelligent Systems and Technology (TIST)* 9, 1 (2017), 1–27.

[10] Yuxi Wang, Kaishun Wu, and Lionel M Ni. 2016. Wifall: Device-free fall detection by wireless networks. *IEEE Transactions on Mobile Computing* 16, 2 (2016), 581–594.

[11] Teng Wei, Shu Wang, Anfu Zhou, and Xinyu Zhang. 2015. Acoustic eavesdropping through wireless vibrometry. In *Proceedings of the 21st Annual International Conference on Mobile Computing and Networking*. 130–141.

[12] Kaishun Wu. 2016. Wi-metal: Detecting metal by using wireless networks. In *2016 IEEE International Conference on Communications (ICC)*. IEEE, 1–6.

[13] Weidong Yang, Xuyu Wang, Anxiao Song, and Shiwen Mao. 2018. Wi-wheat: Contact-free wheat moisture detection with commodity WiFi. In *2018 IEEE International Conference on Communications (ICC)*. IEEE, 1–6.

[14] Zizheng Zhang, Shigemi Ishida, Shigeaki Tagashira, and Akira Fukuda. 2019. Danger-pose detection system using commodity Wi-Fi for bathroom monitoring. *Sensors* 19, 4 (2019), 884.